Deep 3D PALM/STORM imaging: MicAO 3DSR – the key to combining depth and highest resolution

Grégory CLOUVEL, Audrius JASAITIS and Xavier LEVECQ
Imagine Optic, 18 rue Charles de Gaulle, 91400 Orsay, France
contact@imagine-optic.com

APPLICATION NOTE

Summary

The determination of 3D arrangement of cellular structures has become a necessary requirement in cellular biology. Unfortunately, the size of such structures usually lies beyond the diffraction limit and therefore they cannot be visualized in studies using today's widely popular fluorescence microscopy techniques. Photoactivation localization microscopy (PALM) and stochastic optical reconstruction microscopy (STORM) enables us to locate fluorescent molecules with nanometric resolution. Unfortunately in current implementations, these techniques are efficient only in the vicinity of the coverslip, like in total internal reflection (TIRF) or in the first few micrometers inside the sample. Imaging deeper is highly perturbed by the spherical aberration, which is caused by the refractive index mismatch between the sample and immersion oil of the objective. Aberrations can be efficiently corrected using adaptive optics. Here for the correction of aberrations we used MicAO 3DSR – an adaptive optics device containing Shack-Hartman-type wavefront sensor and continuous membrane deformable mirror. By correcting the spherical aberration we can obtain perfectly symmetrical PSF along the Z axis at the depth reaching 50µm in the sample. After the aberration correction, MicAO 3DSR can apply variable amount of astigmatism for three-dimensional imaging. To test the performance of this system for deep PALM imaging we constructed a model sample composed of fixed HeLa cells, stably expressing centrosomal protein centrin-1. For optimization and drift correction, we also added to the sample 100nm fluorescent beads. Our results show that, after correction of aberrations, single molecule imaging can be performed at depths reaching 50µm.

Introduction

Photoactivation localization microscopy (PALM) and stochastic optical reconstruction microscopy (STORM) enable localization of fluorescent molecules with nanometric resolution (Betzig *et al*, 2006; Hess *et al*, 2006; Rust *et al*, 2006). The localization precision in these single molecule localization techniques is highly dependent on the number of detected photons (Thomson *et al*, 2002; Clouvel *at al*, 2013), so maximizing the number of detected photons in these methods is essential. One way to measure this quality is in fact the shape of the Point Spread Function (PSF). The optical components inside the microscope (the high numerical aperture objective, various lenses and dichroic mirrors) and the refractive index mismatch between the immersion oil of the objective and the water based biological sample induce aberrations, which negatively alter the PSF. In addition, depending on the protocol of cell fixation, the biological sample can also induce a pattern of aberrations (Schwertner *et al*, 2007; Simmonds *et al*, 2011), even in the first few hundreds of nanometers from the coverslip. Aberrations affect the symmetry of the PSF in all three dimensions by redistributing the photons from the focal spot to the periphery of the PSF and this way affecting the localization precision (Clouvel *at al*, 2013).

To compensate for these aberrations, Imagine Optic developed an adaptive optics device MicAO 3DSR, specifically designed for 3D PALM/STORM imaging, which can be easily implemented on any inverted frame microscope. Aberrations are detected using image-based modal iterative algorithms (Débarre *et al*, 2007; Facomprez *et al*, 2012) that are simple to use with the integrated MicAO software. The continuous membrane deformable mirror (Mirao 52e) inside MicAO 3DSR is used to correct these aberrations with exceptional precision. After the correction of PSF, the number of detected photons can be almost doubled (Clouvel *et al*, 2013), which leads to significantly improved localization precision in single molecule localization methods (figure 1A and B).

In addition to improved localization precision, MicAO also enables three-dimensional imaging using an astigmatic approach similar to the method based on adding a cylindrical lens (Huang *et al*, 2008). With its deformable mirror, MicAO introduces a tunable amount of perfect astigmatism, free of any residual aberrations (Izeddin *et al*, 2012). An astigmatic PSF is axially asymmetrical, extending in one lateral direction above the focus and in another direction below the focus (figure 1C). The difference between the extension in the X and Y directions reveals how far from the focus the emitter is located. A calibration curve can be generated by recording a Z stack of a diffraction limited point source, for example a small fluorescent bead (smaller than 200nm), and fitting the X and Y widths of the PSF along the Z axis (figure 1D). The most important factor of a high quality calibration curve is the difference between the X and Y width, which ideally forms a straight line (the upper panel of the calibration curve; figure 1D). The slope of this line is indicative of the Z localization precision, which can be tuned by the amount of astigmatism applied by the deformable mirror – the bigger the amplitude of astigmatism, the steeper the slope, and thus the more precise Z localization.

The model sample

As a model of water based sample, we used 200nm fluorescent beads embedded in 2% agarose gel (98% water). Here we show an example z-profile of a 200nm fluorescent bead imaged at 22µm depth (figure 2A). The image-based iterative algorithm (3N) using the deformable mirror corrected for 165nm RMS of spherical aberration, whereas amplitudes of all other Zernike modes were small and therefore could be neglected. After the correction, the fluorescence intensity in the focal plane was almost doubled, the PSF diameter along the Z axis decreased by 50% (the full width half maximum changed from 1639nm to 1172nm) and a symmetrical shape of the PSF above and below the focus was achieved (figure 2B).

An astigmatic approach is completely unusable deeper than 5µm without adaptive correction because the

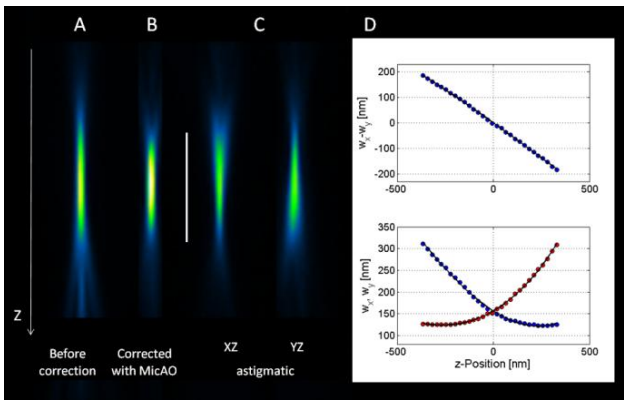

Figure 1. The Point Spread Function on the surface of the coverslip reconstructed from the Z stack of 200nm fluorescent bead (24nm Z step). A. The axial projection of the PSF before correction of aberrations with adaptive optics; B. The axial projection of the PSF after correction of aberrations with MicAO 3DSR; C. The XZ and YZ projections of the PSF with applied 60nm RMS of astigmatism. D. The calibration curve constructed using the data of the astigmatic PSF. The size of the scalebar is 1µm.

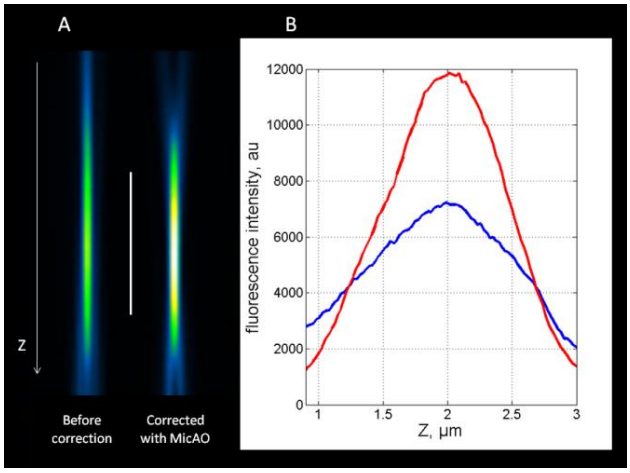

Figure 2. The Z profile of the 200nm fluorescent bead at 22µm depth in 2% agarose. A. Before and after correction of aberrations. The size of the scalebar is 1µm; B. The intensity profile along the Z axis before (blue) and after (red) correction of aberrations. The size of the scalebar is 1µm.

spherical aberration significantly affects the calibration curve due to its axial asymmetry and loss of light. For visualization of this behavior we applied 90nm RMS of astigmatism on the deformable mirror without correcting depth-induced aberrations and imaged the bead at 22µm depth (figure 3A). It can be clearly seen from figure 3A that now the PSF is highly perturbed compared to the PSF on the surface (figure 1). This is especially clear from the calibration curve (figure 3B), which becomes completely asymmetrical, reducing the difference between X and Y extensions of the PSF (the upper panel of figure 3B). However, correction of aberrations completely restores the axial symmetry. As seen in figure 3C, when we corrected for 165nm RMS of spherical aberration and applied 90nm RMS of astigmatism, the PSF became laterally extended as needed above and below the focus, and the resulting calibration curve is perfectly symmetrical.

3D PALM imaging

To demonstrate the feasibility of the astigmatic approach with a deformable mirror for deep 3D PALM/STORM imaging, we used HeLa cells stably expressing the conjugate of mEos2 and centrin1 – one of the proteins from the centrosome complex (Sillibourne *et al*, 2011). Earlier we performed 3D 2-color PALM/dSTORM imaging of two centrosomal proteins, centrin-1 and Cep164 in the close vicinity from the coverslip (Clouvel *et al*, 2013) where we determined the 3D composition of these two proteins with 7nm lateral and 13nm axial localization precision. To perform the 3D deep PALM imaging, we constructed a sample composed of fixed HeLa cells expressing the conjugate of mEos2-centrin1 (kindly provided by James Sillibourne and Michel Bornens, UMR144, Institut Curie, France) embedded in 2% agarose gel at different depths. We also added 100nm fluorescent beads for two purposes: to monitor the lateral and axial drift and to determine the required depth-dependent aberration correction using the 3N algorithm. Here we show the results of PALM imaging at a depth of 50µm.

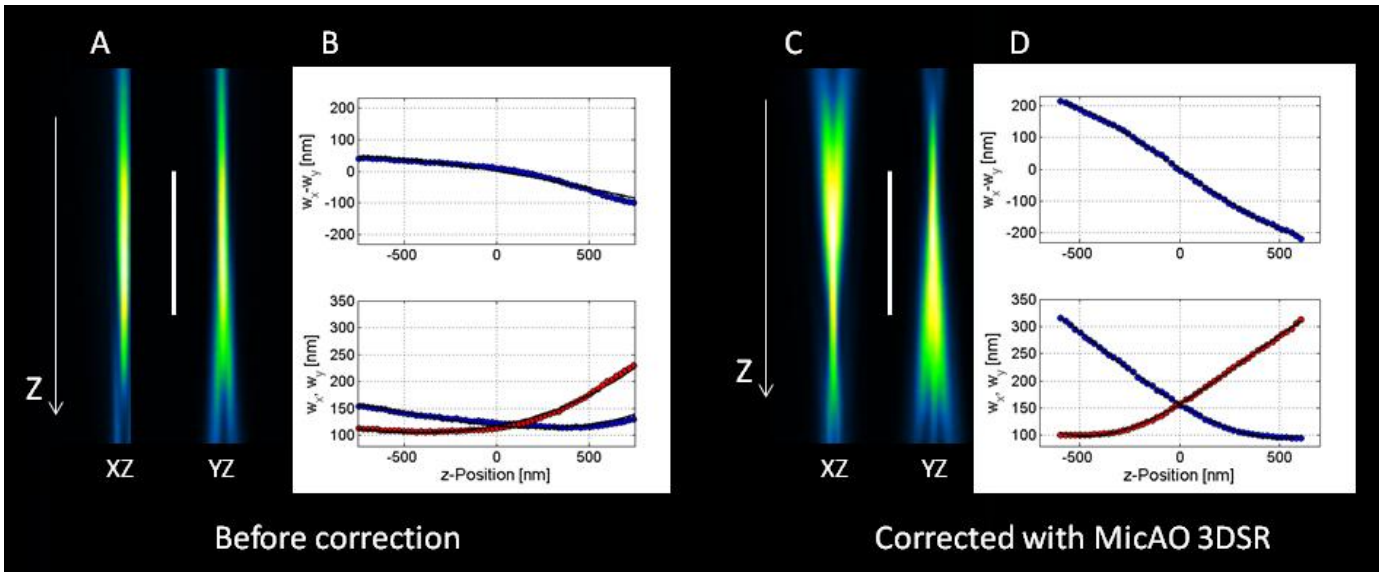

Figure 3. The effect of correction of aberrations at 22µm depth in 2% agarose. A. The XZ and YZ projections of the PSF with applied 90nm RMS of astigmatism before correction of aberrations; B. The calibration curve before the correction; C. The XZ and YZ projections of the PSF with applied 90nm RMS of astigmatism after correction of aberrations with MicAO 3DSR; D. The calibration curve after the correction. The size of the scalebar is 1µm.

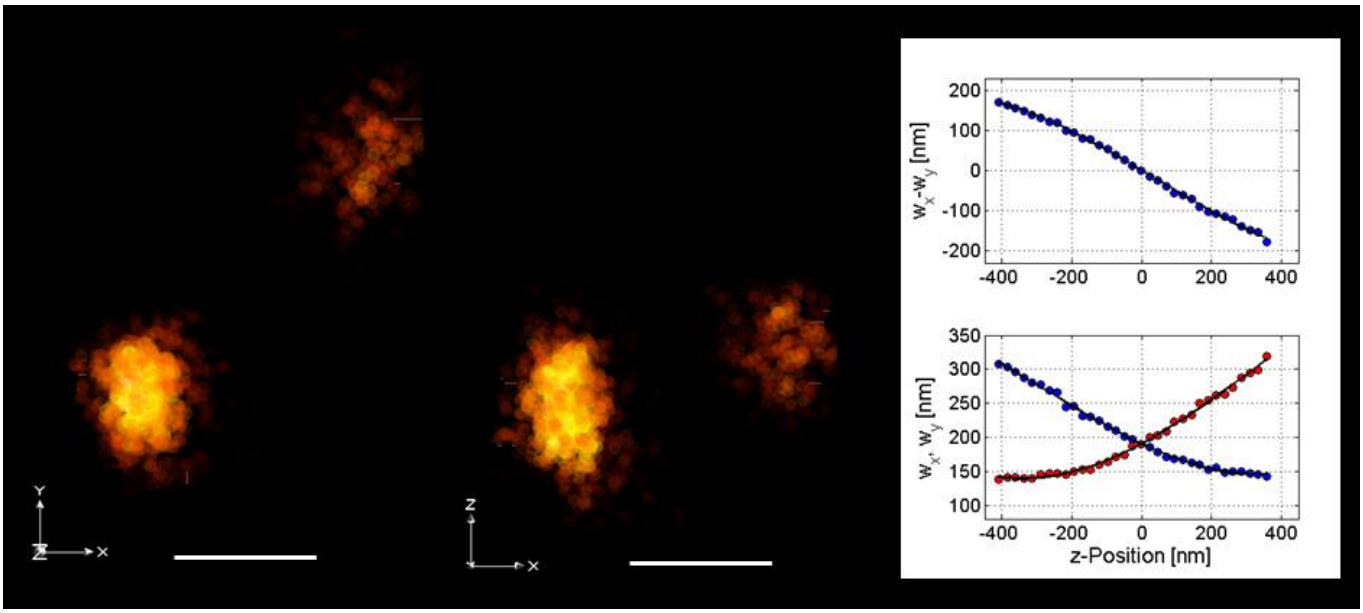

Figure 4. Two projections of mEos2 labeled Centrin1 at 50µm depth in 2% agarose imaged with 3D PALM. The amount of astigmatism induced on the deformable mirror during the imaging was 130nm RMS. The scale bar is 200 nm. For visualization of results we used ViSP software (El Beheiry and Dahan, 2013).

After the correction of aberrations at this depth, we introduced 130nm RMS of astigmatism and acquired the calibration curve (figure 4, right). The slope of this calibration curve is similar to that obtained at the surface of the coverslip, therefore the Z localization precision at 50µm depth is actually comparable to the localization precision on the surface of the coverslip. For the lateral position determination we fitted images with a 2D Gaussian function using an algorithm based on a modified Multi Target Tracking (MTT) algorithm (Sergé *et al* , 2008) as it was described previously (Izeddin *et al*, 2012). Figure 4 shows the reconstructed image of the centrin-1 at 50µm depth. In order to minimize the Z drift we acquired only 3000 frames (1777 localizations) compared to 20000 images taken on the surface (11020 localizations) and the residual Z drift was corrected during the data treatment. The average number of photons was about 500 photons per detection. According to the localization precision dependence on the number of detected photons and to the value of the calibration curve slope (Clouvel *et al*, 2013), the localization precision of this experiment is 13nm laterally and 25nm axially. The precision of the reconstructed structure can also be judged from the size of centrin1 cluster, which is roughly the same as on the surface: the diameter is 100 to 150nm in X and Y and 200nm in Z.

Acknowledgements

We would like to thank James Sillibourne and Michel Bornens (Institut Curie, Paris) for sharing the cell line. We are grateful to Ignacio Izeddin and Xavier Darzacq (Ecole Normale Supérieure (IBENS), Paris), Maxime Dahan and Mohamed El Beheiry (Institute Curie, Paris) for their technical support concerning this application note. Special thanks to Mohamed El Beheiry for the visualization software ViSP. This work was partially funded by the TRIDIMIC project (Agence Nationale de Recherche, ANR).

References

- Betzig E, Patterson GH, Sourgat R, Lindwaser OW, Olenych S, Bonifacino JS, Davidson MW, Lippincott-Schwartz J and Hess HF (2006) "Imaging intracellular fluorescent proteins at nanometer resolution," *Science*, **313**, 1642-1645.
- Clouvel G, Jasaitis A, Sillibourne J, Izeddin I, El Beheiry M, Levecq X, Dahan M, Bornens M and Darzacq X (2013) "Dual-color 3D PALM/dSTORM imaging of centrosomal proteins using MicAO 3DSR," in *Proc. SPIE*, **8590**, 85900Z+.
- Débarre D, Booth MJ and Wilson T (2007) "Image based adaptive optics through optimization of low spatial frequencies," *Opt. Express*, **15**, 8176-8190.

- El Beheiry M and Dahan M (2013) "ViSP: representing single-particle localizations in three dimensions," *Nat. Meth.*, **10**, 689-690.
- Facomprez A, Beaurepaire E and Débarre D (2012) "Accuracy of correction in modal sensorless adaptive optics," *Opt. Express*, **20**, 2598-2612.
- Hess ST, Grirajan TPK and Mason MD (2006) "Ultra-high resolutionimaging by fluorescence photoactivation localization microscopy," *Biophys. J.*, **91**, 4258-4272.
- Huang B, Wang J, Bates M and Zhuang X (2008) "Three-dimensional super-resolution imaging by stochastic optical reconstruction microscopy," *Science*, **319**, 810-813.
- Izeddin I, Beheiry ME, Andilla J, Ciepelewski D, Darzacq X and Dahan M (2012) "PSF shaping using adaptive optics for three-dimensional single-molecule super-resolution imaging and tracking," *Optics Express*, **20**, 4957-4967.
- Rust MJ, Bates M and Zhuang X (2006) "Sub-diffraction-limit imaging by stochastic optical reconstruction microscopy (STORM)," *Nat. Meth.,* **3**, 793-796.
- Schwertner M, Booth MJ and Wilson T (2007) "Specimen-induced distortions in light microscopy," *J. Microscopy*, **228**, 97-102.
- Sergé A, Bertaux N, Rigneault H and Marguet D. (2008) "Dynamic multi-target tracing to probe spatiotemporal cartography of cell membranes," *Nat. Methods*, **5**, 687-694.
- Sillibourne JE, Specht CG, Izeddin I, Hurbain I, Tran P, Triller A, Darzacq X, Dahan M and Bornens M. (2011) "Assessing the Localization of Centrosomal Proteins by PALM/STORM Nanoscopy," *Cytoskeleton* **68**, 619-627.
- Simmonds RD, Wilson T and Booth MJ (2011) "Effects of aberrations and specimen structure in conventional, confocal and two-photon fluorescence microscopy," *J. Microscopy*, **245**, 63-71.
- Thomson RE, Larson DR and Webb WW (2002) "Precise nanometer localization analysis for individual fluorescent probes," *Biophys. J.* **82**, 2775-2783.